Highly ionized atoms in tokamak discharges

E. Hinnov

Plasma Physics Laboratory, Princeton University, Princeton, New Jersey 08540

Tokamak discharges are characterized by electron densities usually $\sim (0.3\text{--}1.0) \times 10^{14}$ cm^{-3} and temperatures from a few hundred eV to several keV. In addition to the working gas (H or He), the plasma normally contains some light impurities ($\sim 10^{12}$ cm^{-3} O or C) that are completely stripped except at the outer periphery, and heavier elements from the vacuum wall and current-aperture limiter (Fe, Cr, Ni, W, Mo, and others, $\sim 10^{10}\text{--}10^{11}$ cm^{-3}) that remain partly stripped, hence relatively strongly radiating, throughout the discharge. Other elements, especially noble gases, may be deliberately added for diagnostic purposes. Resonance lines of Fe and Ar in the beryllium and lithium sequences, of Fe, Kr, and Mo in the magnesium and sodium sequences, and of Mo and Xe in the zinc and copper sequences have been used for rough determination of plasma composition. Since crucial plasma characteristics such as temperature and confinement time are sensitively affected by the local composition, it is essential to improve the available atomic data necessary for more accurate analysis: wavelengths, transition probabilities, excitation, ionization, and recombination rates, especially for the heavier elements.

I. INTRODUCTION

The tokamak discharge produces plasmas that can vary over a considerable range in electron temperature T_e, both in space and time in a given discharge, and in discharges of different initial or boundary conditions. For the purpose of producing light of highly ionized atoms, it is the highest central temperatures that are of primary interest. These vary in present-day tokamaks from about 1.5 to 3 keV, i.e., roughly comparable to temperatures reached in solar flares. The other parameter of interest in producing highly ionized atoms is the product of electron density n_e and the ion confinement time τ, which reaches values of $n_e\tau \approx (1\text{--}3) \times 10^{12}$ sec/cm^3 in the discharges described in the present paper. The highest state of ionization reached by a given atom is determined either by this product or by the inverse rate coefficient of recombination at the ambient temperature, whichever is smaller. Generally, plasmas of highest temperature also have the longest confinement times, but the study of highly ionized atoms is complicated by the fact that their presence in sufficient quantities to be observable also affects adversely the achieved temperatures and confinement times.

The working gas that provides the bulk of the plasma is usually hydrogen or deuterium, sometimes helium. The plasma generally contains several percent oxygen and lesser amounts of carbon desorbed from the walls. These affect the plasma behavior considerably, but they are not of direct concern in the present paper. The heavy atoms under discussion are (1) those of stainless-steel vacuum walls, and molybdenum current-aperture limiters, that are released by

sputtering or evaporation during the discharge, and (2) atoms of noble gases deliberately introduced in controlled quantities for diagnostic purposes. In this paper we report the measurement of wavelengths and intensities, and the identification of the electronic transitions, for several resonance lines of highly ionized states of these atoms.

II. EXPERIMENTAL SETUP

The light source used in the present work was the Princeton ST Tokamak. Since the operation of tokamaks generally,[1] and also of the ST tokamak,[2-4] have been amply discussed in recent literature, we shall confine the description of the discharge only to such features that are directly relevant to the observation of the highly ionized ion resonance lines.

The plasma is produced in a toroidal magnetic field, within a stainless-steel vacuum vessel of 15.8 cm minor and 109 cm major radius by a toroidal current I_{OH}, in an initial working gas (H$_2$ or He) density of about 10^{13} cm^{-3}. At one toroidal position a heavy rectangular (usually 12×13 cm^2) molybdenum aperture limits the current dimensions and reduces the interaction between hot plasma and the vacuum vessel.

Typical behavior of a discharge is shown in Fig. 1. The heating current I_{OH} rises within a few milliseconds to about 60 kA, and thereafter increases slowly to a flat maximum of about 80 kA some 60–70 msec later. The average electron density (number per cm^2 along the line of sight in the equatorial plane of the torus, divided by the limiter aperture) rises very rapidly to an initial peak, and varies slowly thereafter, either rising slowly as in Fig. 1 or perhaps falling slowly under some
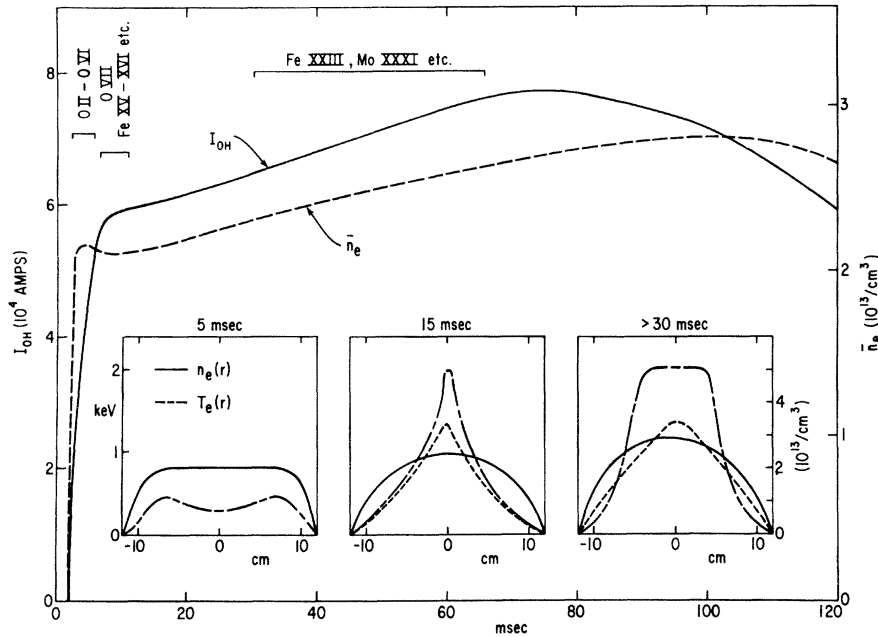
FIG. 1. Typical time evolution of electron density and temperature is an ST tokamak discharge. Dashed curves in the insets describe alternative temperature evolutions, as discussed in the text.

other discharge conditions. The electron density behavior is determined by approximate balance between particle loss by diffusion, etc., and continued ionization of the recycled particles, i.e., those neutralized on the walls or the limiter returning to the plasma. The average confinement time, i.e., the characteristic time a given atom stays in the plasma, is only a few milliseconds in the early phase and perhaps 15–20 msec in the quasisteady part of the discharge. The confinement time appears to be at least approximately the same for all plasma constituents: electrons, protons, and the various impurity ions.

The insets in Fig. 1 describe the radial distributions of electron density and temperature at different times during the discharge. In the early phase, ~5 msec on the scale of the main figure, the electron density is usually fairly uniform, although various fine structures may occur under some conditions. The electron temperature may have risen to 300–400 eV, and often shows a radial shell structure as indicated, caused by the current skin effect. About 10 msec later the density profile has become approximately parabolic; this shape, with perhaps minor modifications, persists throughout the rest of the discharge. The electron temperature distribution at around 15 msec has developed a peaked profile with a height of perhaps 2 keV or more, and the peak subsequently broadens to a flat plateau, with a width of 6–8 cm, but the profile remains considerably narrower than the density profile, i.e., there is a hot plasma core surrounded by a considerably

cooler plasma of similar density. An alternative temperature profile development is depicted by the dotted curves: here the central temperature fails to grow beyond about 1.5 keV and, although it may broaden somewhat in time, tends to retain a roughly triangular shape. This latter distribution development is associated with higher concentrations of heavy impurities, either wall materials or added elements. A high state of ionization of a given element may thus be unobservable because there is either too little of the element present or too much, and the conditions of optimum observability are often difficult to establish.

The resonance lines of the first five states of oxygen appear successively during the first few milliseconds of the discharge, go through pronounced maxima during the time indicated in Fig. 1 (some samples are presented below), and subside to quasisteady plateaus of intensity that originate from the outer periphery of the plasma, where the electron temperature is comparable to the ionization potential of the ion in question, i.e., ≤100 eV. From about 7 to 12 msec appear qualitatively similar lines of ions of ionization potential of several hundred eV, such as Mo XIII and XIV, Fe XV and XVI, O VII, and others. Finally, at times of ~30 msec and later, there appear the lines of the highly ionized atoms that constitute the main topic of this paper.

The line intensities were measured with a Spex 1-m vacuum monochromator equipped with a Jobin-Yvon holographically ruled gold-coated

1200-groove/mm grating at 83° angle of incidence, and Bendix magnetic electron multiplier with tungsten cathode. The instrumental bandwidth was approximately 1 Å, determined by the width of the slits. The quoted wavelengths are accurate to ± 0.5 Å in the case of stronger lines that could be clearly distinguished from continuum emission and neighboring lines and scattered light, principally due to oxygen. The instrument was calibrated *in situ* by means of the line-ratio method,[5] with results shown in Fig. 2. Each of the measured points is reproducible to about 20% or better. The points represented by neutral helium lines are only slightly affected by self-absorption because at the time of measurement the emission line is much wider than the absorption line, due to resonant charge-exchange collisions in the plasma.[6] The points at $L\alpha$ and He II 256–304 Å are based on calculated relative populations of the $n = 2$–4 levels.[7] These calculations are probably better than the measurement accuracy, except for the case of the $\lambda 304$-Å line, where the indicated spread is due to the uncertainty of electron temperature at the time of measurement. The interpolated curve is then used to measure the unknown line intensities. Fortunately, most of the lines discussed in this paper are not very far from measured points.

The intensities are measured as surface brightness, number of photons per sec cm² sr, in the midplane of the torus. At the time of peak inten-
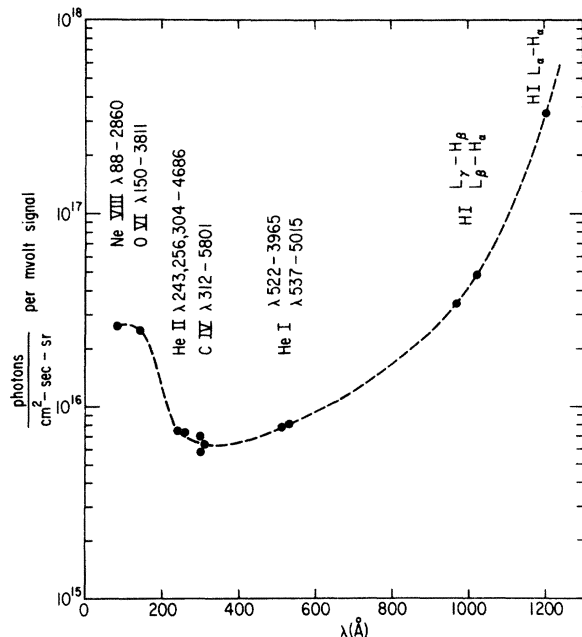
sity, the local emissivity is given by multiplying the brightness by $4\pi/\Delta r$, with $\Delta r \approx 20$–24 cm for the early states of ionization, during the first several milliseconds of the discharge, where $n_e(r)$ and $T_e(r)$ are fairly flat, and $\Delta r \approx 6$–8 cm for the higher states of ionization, corresponding to the narrow high-temperature part of the discharge. The drop of the intensity after the maximum, while the electron density and temperature are steady or increasing, then indicates decrease of the effective Δr, usually by ionization to the next state near the center of the plasma and the consequent development of the cylindrical shell structure of the radiation mentioned above.

III. RESULTS

The deliberately added elements, such as the noble gases, provide important advantages in identification of the lines: the element is *a priori* known, and the amount can be adjusted for optimum observation conditions. We therefore discuss these cases first.

(a) Krypton. The data obtained in a discharge with an initial gas filling of deuterium (6.6×10^{12} D_2 molecules/cm³) with 2.9×10^{10} atoms/cm³ of krypton are given in Fig. 3, and the early part of the discharge with expanded time and contracted intensity scales is shown in Fig. 4.

The early electron density is roughly double that of the initial D atom density. This is almost entirely due to the ratio of the vacuum vessel volume to plasma volume. The contribution of other constituents, even of oxygen, is small at this time, and remains rather modest even at later times. The variation of $\bar{n}_e$ in time is determined almost entirely by plasma confinement and recycling and thus only indirectly (through electron temperature, electrical resistivity, etc.) through composition.

The central temperature rises nearly linearly to 1.5 keV and thereafter levels off. However, from about 60–70 msec there is a somewhat unusual additional rise to about 1.9 keV, which may be associated with a substantial part of the krypton in the center reaching the neonlike configuration and thereby decreasing its radiation efficiency.

In discussing the radiation, we note that in the case of all the spectrum lines mentioned in this paper, the lines are emitted from a plasma at an electron temperature such that

$$kT_e \approx E_i \gg E_x, \qquad (1)$$

where E_i is the ionization potential of the ion in question and E_x is the excitation potential for the line. Furthermore, the various, relevant transi-

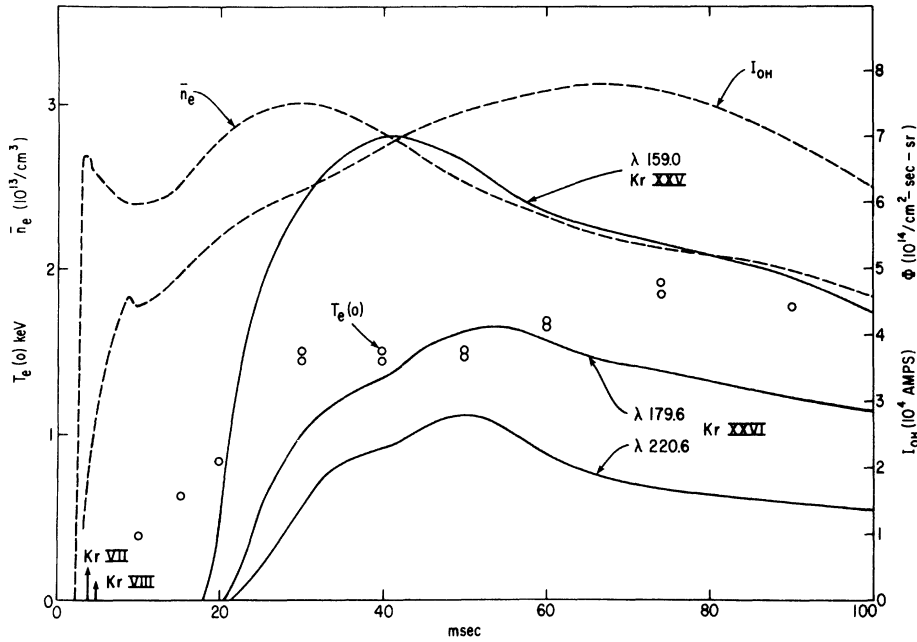FIG. 2. Reciprocal sensitivity of the uv monochromator, and the line pairs used for calibration.

FIG. 3. Heating current, average electron density, central electron temperature (○), and intensities of Mg- and Na-sequence krypton resonance lines vs time. The arrows indicate times of appearance of Zn- and Cu-sequence krypton lines shown in Fig. 4.

tion rates are such that the line emission is almost exclusively due to electron collisional transitions from the ground state of the ion (lower state of the transition), followed by spontaneous radiative deexcitation. Under these conditions the line intensity is very nearly independent of T_e, and also depends very weakly on the near-threshold excitation cross-sections or effective Gaunt factors,[8-10] and scales as

$$\bar{\Phi} \propto f/E_x^{3/2} \propto f\lambda^{3/2} , \qquad (2)$$

with f the absorption oscillator strength and λ the wavelength for the line. The observed intensity variations are then due to the variation of the particular state of ionization of the atom (along the line of sight) and the nearly constant electron density.

Kr VII and Kr VIII lines peak at a time when the electron temperature has reached about 100–130 eV (comparable to the ionization potentials 111 and 123 eV, respectively). The oxygen ions O V (E_i = 114 eV) and O VI (E_i = 138 eV) peak slightly later.
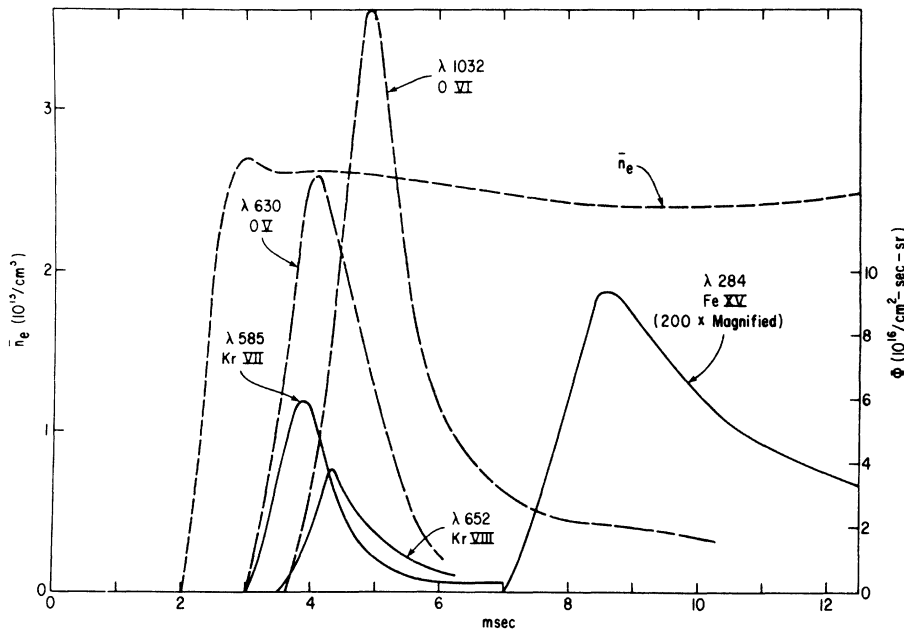

FIG. 4. Time behavior of electron density and intensities of the earlier states of ionization of krypton and of oxygen and iron in the early part of the discharge of Fig. 3. Note the change of intensity scale, except for the iron line, which is in the same scale as in Fig. 3.

The delay may be due to initial conditions: oxygen is injected mostly as desorbed water vapor during the first millisecond or so of the discharge, whereas krypton presumably occupies the volume from the start. An interesting feature is the inversion of the relative intensities: the $2s^2$-$2s2p$ singlet line of O V is weaker than the $2s\,^2S_{1/2}$-$2p\,^2P_{3/2}$ line of O VI (almost exactly the same relationship has been recently observed in the tokamak of the Fontenay-aux-Roses[11]), whereas the reverse is true of the $n = 4$ transitions in krypton. Aside from experimental uncertainties, there are two probable causes for this phenomenon. According to the best available theoretical cross-section, the rate coefficients for excitation[11] of the O V and O VI lines at about 100 eV electron temperature are 2.8×10^{-8} and 1.7×10^{-8} cm^3/sec, respectively, whereas an adaption of the same procedure of calculation for the Kr VII and Kr VIII lines (also used for other lines quoted below) gives 5.5×10^{-8} and 2.4×10^{-8} cm^3/sec, respectively. Another and perhaps more important question in the intensity inversion is the relative importance of the triplet $nsnp\,^3P$ populations relative to the singlet ground state. It appears from a comparison of singlet- and triplet-line intensities of O V that about half or slightly more of the O V population is in the triplet state at the electron densities and temperatures in question, which incidentally explains why the O V line is weaker than the O VI line with its smaller excitation rate coefficient. Corresponding information about the triplet in Kr VII is unfortunately not available, but the intensity relationship with Kr VIII suggests that the proportion of triplets here is relatively less. This, and analogous problems in other elements, particularly those with ns^2 ground configurations, evidently needs further investigation.

Another possible explanation of the intensity changes would be a rapid increase of the relative oxygen concentration or decrease of krypton concentration in time. However, other evidence, including the subsequent behavior of the discharge,[2,12] and the soft x-ray continuum and krypton K-line intensity,[4] indicates that this is not the case—the relative concentrations change only very slowly, if at all, on the time scale of the discharge.

The $\lambda284$-Å Fe XV ($E_i = 456$ eV) line appears at a time when the central electron temperature exceeds 300 eV, as expected from the rates of ionization. The excitation rate coefficient for this line is about 10^{-8} cm^3/sec.

Similar calculations for the appearance of the magnesiumlike Kr XXV ($E_i = 1151$ eV) and sodium-like Kr XXVI ($E_i = 1206$ eV) indicate that they should appear at between 20 and 30 msec on the time scale of Fig. 3. The approximate location

of the resonance lines of these ions were extrapolated from known lines of the isoelectronic sequences by a procedure described by Edlén,[13] and a search in the neighborhood of the predicted lines yielded the three lines shown in Fig. 3. The limit of sensitivity was about a factor of 2–3 below the intensity of the 221-Å line, and within this limit no other krypton line of similar time behavior (i.e., of the same or nearby states of ionization) were found between 130 and 250 Å. We therefore have little doubt about their identification: $\lambda159.0$-Å Kr XXV $3s^2\,^1S$-$3s3p\,^1P$, and $\lambda\lambda179.6$-, 220.6-Å Kr XXVI $3s\,^2S$-$3p\,^2P_{3/2,1/2}$, respectively. The predicted rate coefficients for excitation are 2.6×10^{-9} cm^3/sec for the $\lambda159$-Å line/and 1.6×10^{-9} for the sum of the other two, at 1.5 keV temperature. These numbers are in reasonable agreement with the relative intensities, again considering that some of the Kr XXV population should be in the triplet state. The ratio of the Kr XXVI lines appears to vary in time from about 1.6 early to 2.0 late in the discharge, but this is probably due to difficulties in allowing for background radiation, which is in intensity comparable to the weaker line, especially in later part. According to the $f\lambda^{3/2}$ scaling, the expected ratio using the f values of Weiss and Wiese[14] should be 1.8, in reasonable accord with observation.

Compared to the earlier Kr VII and VIII lines, the Kr XXV and XXVI line intensities are weaker by a factor of 80–90. Most of this, a factor of 20–25, is ascribed to the excitation rate coefficients quoted above, and the rest, about a factor of 4, to the shortening of the path length Δr along the line of sight where the radiation originates, according to the temperature profiles explained in Fig. 1. In other words, the quoted rate coefficients for excitation are consistent with the assumption of no significant change in time of the relative proportion of krypton in the plasma composition.

(b) Xenon. The appearance of the xenon lines $\lambda164.5$ Å, ascribed to $4s^2\,^1S$-$4s4p\,^1P$ of Xe XXV, and $\lambda\lambda173.9$, 234.2 Å, ascribed to $4s\,^2S$-$4p\,^2P_{3/2,1/2}$ of Xe XXVI, are shown in Fig. 5. The hydrogen pressure and heating current were about the same as in the krypton case, but the Xe initial pressure was higher, about 9×10^{10} atoms/cm^3. This was sufficient to significantly depress the electron temperature, which reached only about 800 eV at 20–30 msec. As a consequence of the lowered temperature, the particle confinement time also was smaller and resulted in lower electron density. Nevertheless, the Xe XXV and Xe XXVI ions are readily produced because of their relatively low ionization potentials (853 and 891 eV, respectively). The only qualitative difference from the
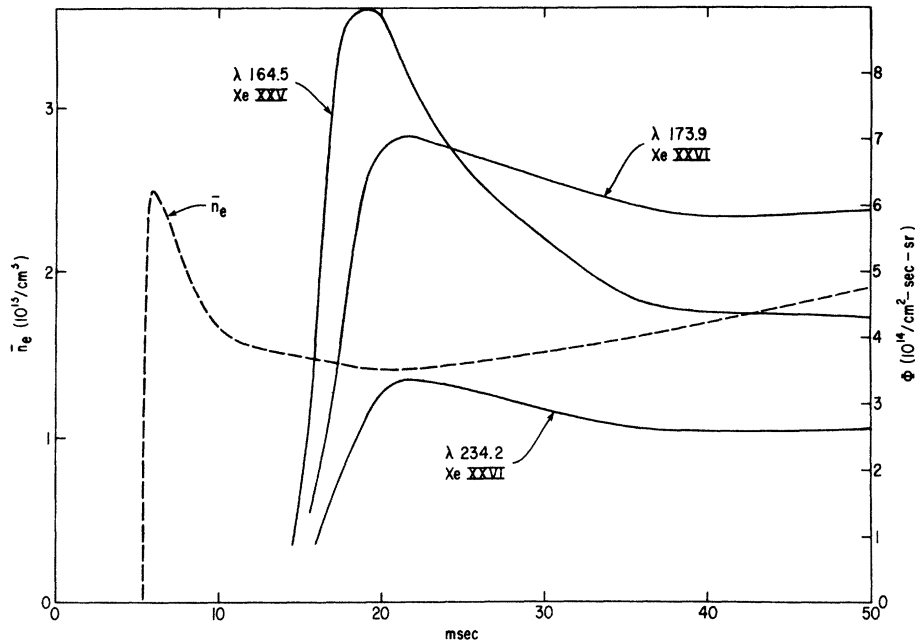
FIG. 5. Time behavior of the Zn- and Cu-sequence resonance lines of xenon and the average electron density.

krypton lines is the relatively higher intensity of the $\lambda 174$-Å ^2S-$^2P_{3/2}$ line with respect to both $\lambda 234$- and $\lambda 165$-Å lines.

The copper-sequence wavelengths are in good agreement with recent relativistic Hartree-Fock calculations (173.4, 233.7 Å at Systems, Science, and Software[15] and 180.8, 237.3 Å at the U. S. Natl. Bur. Stand.[16] The latter reference also includes calculation of oscillator strengths, according to which the line ratio should again be 1.8, somewhat smaller than the measured ratio of about 2.1.

(c) *Argon.* An analogous experiment with 2.2×10^{10}-cm^{-3} argon added to hydrogen discharge yielded the following intensities and wavelengths at a time when $\bar{n}_e = 1.4 \times 10^{13}$, $T_e(0) = 1.2$ keV. For $2s^2$-$2s2p$ Ar XV ($E_i = 855$ eV), the intensity was 5.5×10^{14}/cm^2 sec sr and $\lambda = 221.2$ Å; for $2s$-$2p$ Ar XVI ($E_i = 918$ eV), the intensities were 4.1 and 2.5×10^{14} for $\lambda 354.1$- and 389.3-Å lines, respectively. These lines had been identified previously,[17,18] and their wavelengths agree with the published values to well within experimental uncertainty.

(d) *Iron.* The observation of identifiable lines of highly ionized wall or limiter materials in the tokamak discharge is considerably more difficult than that of the added noble gases, partly because of less control over the amounts, and partly because of higher relevant ionization potentials and the consequent critical balance between the required temperature and the amount of the heavy element. One characteristic of the iron (and perhaps also of molybdenum) concentration is that it generally does not appear to remain a constant fraction of the discharge, such as krypton or

oxygen, but tends to vary, and usually to increase, slowly in time. This behavior is probably due to a different release mechanism (evaporation or sputtering rather than desorption or direct recycling) and not to different confinement properties of these atoms.

The observed iron resonance line intensities in a discharge where the total iron concentration appears to rise somewhat more rapidly than usual are shown in Fig. 6, together with a Mo XIII line. Compared with the discharges discussed above, the limiter radius was increased from 12 to 13 cm, i.e., closer to the stainless-steel vacuum-vessel radius, the initial hydrogen density was slightly less, and the heating current was increased to a peak of 100 kA (at about 60–80 msec). The electron temperature was not monitored in detail, but comparison with similar conditions in other occasions suggests that the central temperature rose to somewhat above 2 keV at about 25 msec and dropped slowly thereafter to the 1.7–1.8 values shown at 60–80 msec, with the radial profile flattened to perhaps 6–8 cm, as indicated in Fig. 1. The continued increase of the Fe XV line after 30 msec [which line at that time originates in an approximately cylindrical shell at a radial location where $T_e(r) \approx 300$ eV] is an indication of iron influx rate, rather than of density directly. However, if the ion confinement time remains approximately constant in time, it is also a rough measure of total iron density increase in time. (Note that the concurrent change of electron density does not substantially affect the intensity in the shell, since both the local excitation and ion-
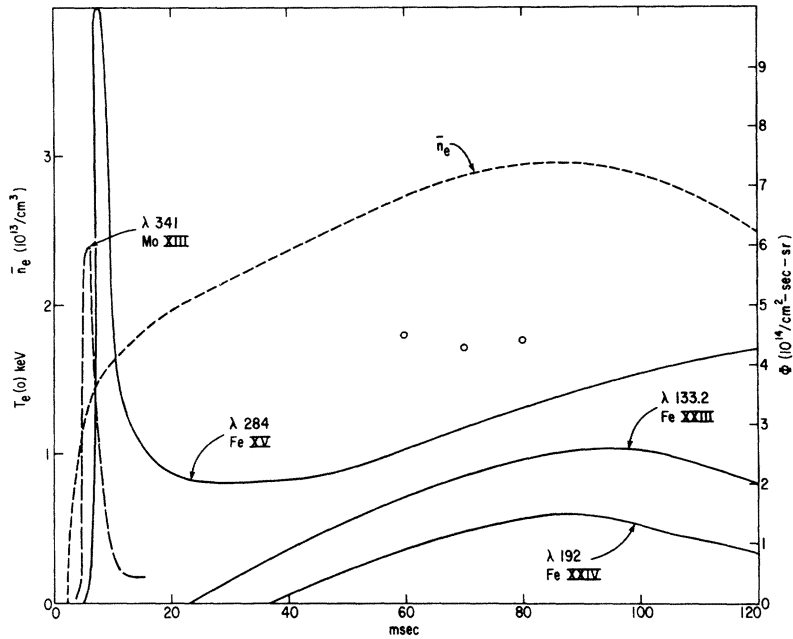
FIG. 6. Time behavior of the Mg-, Be-, and Li-sequence iron resonance lines and the average electron density with peak electron temperatures at 60–80 msec (O), and appearance of the Mo XIII resonance line, in a hydrogen discharge.

ization rates are proportional to the electron density. See Ref. 11 for a detailed discussion of the radiation emissions.)

The strongest late-appearing line at $\lambda 133.2$ Å is ascribed to the $2s^2\,{}^1S\text{-}2s2p\,{}^1P$ transition of Fe XXIII, and the $\lambda 192$-Å line is ascribed to the $2s\,{}^2S\text{-}2p\,{}^2P_{3/2}$ transition of Fe XXVI. Another line at about 256 Å with similar time behavior and approximately one-half the intensity of $\lambda 192$-Å line must be the second component of the doublet. In the latter two, and especially in the $\lambda 256$-Å case,

the accuracy is only about ± 1 Å because of the difficulties of distinguishing the relatively small and slowly varying intensities from the background radiation. All three of these lines have been identified in solar-flare spectra.[18-21]

The approximate expected rate coefficients for excitation at 1.8 keV are 5.0 and 3.7×10^{-10} cm^3/sec for the $\lambda 133$- and $\lambda 192$-Å lines are in reasonable agreement with the observed relative intensities. Comparison with the $\lambda 284$-Å line and its expected rate coefficient 1×10^{-8} cm^3/sec at
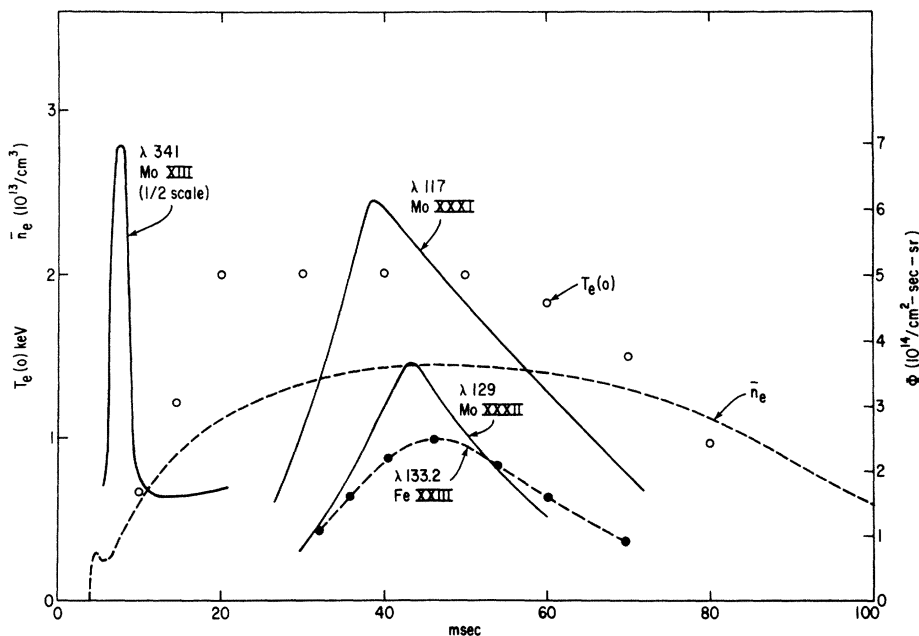

FIG. 7. Time behavior of the Zn-, Mg-, and Na-sequence molybdenum resonance lines, the Fe XXIII line, and the average electron density and peak temperature (O) in a hydrogen discharge. The Mo XIII line intensity is double the value shown in the figure.

300 eV and taking into account the increased elec-
tron density indicates an increase of about a factor
of 3 in the iron concentration from 8 to 70 msec.
This is consistent with the observed increase of
the $\lambda284$-Å line intensity in time, but detailed
measurements of spatial distributions of the light
are essential for quantitative conclusions on the
ion accumulation rate.

(e) Molybdenum. The results of a discharge
that favors molybdenum rather than iron lines
are shown in Fig. 7. Here the limiter radius was
again 12 cm, the initial hydrogen pressure was
lower, and the discharge contained relatively
more oxygen than in the preceding case. The re-
lative intensities of $\lambda341$-Å Mo XIII (peak at 1.4
$\times10^{15}$/cm^2 sec sr) and $\lambda284$-Å Fe XV (not shown)
are approximately reversed compared to Fig. 6.
The strongest late-appearing lines, $\lambda117$ and
$\lambda129$ Å, are ascribed to the $3s^2\,{}^1S$-$3s3p\,{}^1P$ transi-
tion of Mo XXXI ($E_i = 1805$ eV) and the $3s\,{}^2S$-$3p\,{}^2P_{3/2}$
transition of Mo XXXII ($E_i = 1896$ eV). The other
line of the doublet appears to be 177 Å, but the ob-
servation is somewhat uncertain because of rela-
tively strong oxygen lines in the vicinity.

The times of appearance and the relative inten-
sities of these lines are consistent with this identi-
fication, and so is the relationship to the Fe XXIII
($E_i = 1930$ eV) line. The intensity relationship of
the $\lambda117$-Å line to the $\lambda341$-Å Mo XIII line is about
the same, taking into account the different elec-
tron density change as in the corresponding iron
case ($\lambda284$ vs $\lambda133$ Å in Fig. 6). This might be
expected on the basis of the estimated excitation
rate coefficients (2×10^{-8} cm^3/sec for $\lambda341$ Å at
300 eV, 1.2×10^{-9} for $\lambda117$ Å at 2 keV).

The principal reason for questioning the identifi-
cation is the appearance of a strong feature in the
solar-flare spectrum at 117 Å ascribed[20] mainly
to the ${}^2P_{1/2}$-${}^2S_{1/2}$ resonance line of Fe XXII (E_i
$= 1794$ eV). Since iron is definitely present in
the tokamak discharge, and the appearance time
for the Fe XXII line should be very similar to
that determined from our observations, the dis-
tinction can be made only on the basis of intensity.
The berylliumlike and lithiumlike spectra of iron
seem to be relatively stronger in the tokamak dis-
charge than in the flare spectrum[20]—none of the
other lines of Fe XIX–XXII could be clearly dis-
tinguished from the background. Therefore the
observed relative strength of $\lambda117$–$\lambda133$-Å lines
can hardly be explained by ascribing the former
to Fe XXII alone. Furthermore, in different ex-
periments, such as those shown in Figs. 6 and 7,
the $\lambda117$-Å line appears to correlate with molyb-
denum, rather than with iron concentrations.

Both $\lambda117$ and $\lambda129$-Å lines have been observed
subsequently in the TFR tokamak,[11] but because

of the basic similarity of the devices, the identifi-
cation problems are also similar. Perhaps strong-
er support comes from recent Hartree-Fock cal-
culations[16] that show good agreement with our
wavelengths. On the balance we think the identifi-
cations to be fairly solidly based. Of course, this
does not negate the existence of the Fe XXII line,
but asserts that its contribution to the measured
intensity in the tokamak discharge is minor.

Other molybdenum lines, of earlier states of
ionization, that have been measured in ST tokamak
discharges are shown in Fig. 8. The identification
of the three strongest lines is fairly certain, as
they require only a short extrapolation from
known sequences, and their time behavior and
relative intensities are as expected. The transi-
tions of the weaker lines are unidentified; the
ionization states are ascribed on the basis of time
of appearance.

IV. SUMMARY

The wavelengths and identifications of the ob-
served lines are given in Table I. The iron and
argon lines have already been identified in solar
flares,[17-21] and some of the molybdenum lines in
tokamak discharges have been reported before.[2]
The identifications are based on (a) changing the
plasma composition to determine the element, (b)
comparing the observed time behavior of the in-
tensity with approximate calculations based on
known or estimated rate coefficients at the ap-
propriate electron temperatures and densities,
and (c) comparison with extrapolated isoelectron-
ic sequences. In most cases there are also recent
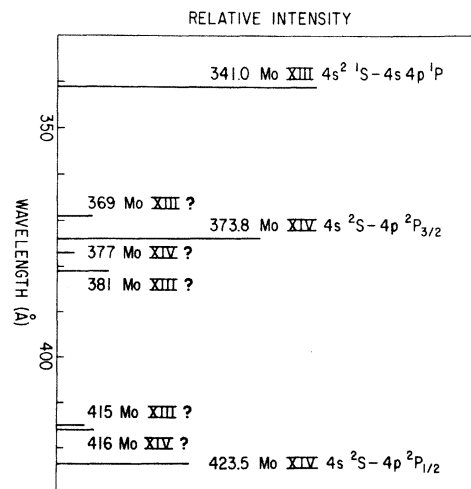*ab initio* calculations available for comparison.

FIG. 8. Wavelengths and relative intensities of several
Mo XIII and XIV lines.

TABLE I. Wavelengths and transitions of the lines observed in the ST tokamak.

Ion	Transition	Wavelength (Å)	Sequence
Xe xxv	$4s^2 {}^1S - 4s4p\ {}^1P$	164.5	Zn
Mo xiii	$4s^2 {}^1S - 4s4p\ {}^1P$	341.0	Zn
Xe xxvi	$4s\ {}^2S - 4p\ {}^2P_{3/2,1/2}$	173.9, 234.2	Cu
Mo xiv	$4s\ {}^2S - 4p\ {}^2P_{3/2,1/2}$	373.8, 423.5	Cu
Mo xxxi	$3s^2 {}^1S - 3s3p\ {}^1P$	117.0	Mg
Kr xxv	$3s^2 {}^1S - 3s3p\ {}^1P$	159.0	Mg
Mo xxxii	$3s\ {}^2S - 3p\ {}^2P_{3/2,1/2}$	129, 177	Na
Kr xxvi	$3s\ {}^2S - 3p\ {}^2P_{3/2,1/2}$	179.6, 220.6	Na
Fe xxiii	$2s^2 {}^1S - 2s2p\ {}^1P$	133.2	Be
Ar xv	$2s^2 {}^1S - 2s2p\ {}^1P$	221.2	Be
Fe xxiv	$2s\ {}^2S - 2p\ {}^2P_{3/2,1/2}$	192, 256	Li
Ar xvi	$2s\ {}^2S - 2p\ {}^2P_{3/2,1/2}$	354.1, 389.3	Li

(Because of some possibilities of interfering lines of Fe, Cr, or Ni ions at states of similar ionization potential, the identification of the Mo XXXI and XXXII lines should perhaps be regarded as tentative until some independent confirmation is obtained.) The measured wavelengths are accurate to ± 0.5 Å in the cases where the decimal is shown and to ± 1 Å where it is not. The measured intensities have given useful information about relative intensities of doublets, and also of lines of adjacent states of ionization. In the case of added noble gases, the known amounts and measured intensities allow the deduction of rate coefficients for excitation, which in turn can be used to evaluate the amounts of spontaneously occurring elements from measured intensities of analogous transitions.

The accuracy of such deductions of concentration is adequate to establish the order of magnitude of the various plasma constituents and estimate their overall influence on the plasma behavior, e.g., their probable contributions to electrical resistivity and local energy loss by radiation. However, it is not satisfactory for finer detail, such as the important problem of the accumulation rate of heavy ions in the discharge. Improvement in this situation must be sought in two directions, experimentally by providing radial distributions of the line emissivities and more detailed and accurate intensity measurement calibrations, and theoretically by providing transition probabilities and rate coefficients for excitation of the appropriate lines and of ionization and recombination of the ions that can be relied on at least to 20–30%.

[1] H. P. Furth, Nucl. Fusion 15, 487 (1975).
[2] D. L. Dimock et al., Plasma Physics and Controlled Nuclear Fusion Research (Proceedings of the Fourth International Conference, Madison, 1971) (IAEA, Vienna, 1971), Vol. 1, p. 451.
[3] D. L. Dimock et al., Nucl. Fusion 13, 271 (1973).
[4] S. von Goeler et al., Nucl. Fusion 15, 301 (1975).
[5] E. Hinnov and F. W. Hofmann, J. Opt. Soc. Am. 53, 1259 (1963).
[6] J. G. Hirschberg and E. Hinnov, J. Chem. Phys. 45, 2233 (1966).
[7] L. C. Johnson and E. Hinnov, J. Quant. Spectrosc. Radiat. Transfer 13, 333 (1973).
[8] B. L. Moiseiwitsch and S. J. Smith, Rev. Mod. Phys. 40, 238 (1968).
[9] O. Bely, Proc. Phys. Soc. Lond. 88, 587 (1966).
[10] J. Davis, J. Quant. Spectrosc. Radiat. Transfer 14, 549 (1974).
[11] Equipe TFR, Nucl. Fusion 15, 1053 (1975).
[12] N. Bretz et al., Nucl. Fusion 15, 313 (1975).
[13] B. Edlén, Encyclopedia of Physics, edited by S. F. Flugge (Springer, Berlin, 1964), Vol. XXVII, p. 80.
[14] A. W. Weiss and W. L. Wiese, Bull. Am. Phys. Soc. 20, 1295 (1975).
[15] D. E. Parks (private communication).
[16] A. W. Weiss (unpublished).
[17] B. C. Fawcett et al., J. Phys. B 4, 986 (1971).
[18] J. D. Purcell and K. G. Widing, Astrophys. J. 176, 239 (1972).
[19] S. O. Kastner, W. M. Neupert and M. Swartz, Astrophys. J. 191, 261 (1974).
[20] B. C. Fawcett and R. D. Cowan, Mon. Not. R. Astron. Soc. 171, 1 (1975).
[21] K. G. Widing, Astrophys. J. 197, L33 (1975).